BIOCHEMISTRY

 Volume 44, Number 21 May 31, 2005

*Articles*

# Structural and Biochemical Characterization of Gun4 Suggests a Mechanism for Its Role in Chlorophyll Biosynthesis[†,‡]

Paul A. Davison,[§,||] Heidi L. Schubert,[*,§,⊥] James D. Reid,[||] Charles D. Iorg,[⊥] Annie Heroux,[#] Christopher P. Hill,[⊥] and C. Neil Hunter[*,||]

*Department of Molecular Biology and Biotechnology, University of Sheffield, Sheffield S10 2TN, U.K., Department of Biochemistry, University of Utah, Salt Lake City, Utah 84132, and Department of Biology, Brookhaven National Laboratory, Upton, New York 11973-5000*

*Received February 9, 2005; Revised Manuscript Received March 22, 2005*

ABSTRACT: Gun4 has been implicated in a developmental signaling pathway between the chloroplast and the nucleus involving magnesium protoporphyrin IX ($MgP_{IX}$), the first dedicated intermediate in the chlorophyll biosynthetic pathway. Here we present the crystal structure of *Thermosynechococcus elongatus* Gun4 at 1.5 Å, describe the binding affinities of Gun4 for substrate and product porphyrin molecules, and identify a likely $(Mg)P_{IX}$ binding site on the protein. Kinetic analyses show that Gun4 dramatically increases the efficiency of transformation of porphyrin substrate to metalloporphyrin product and that it also reduces the threshold $Mg^{2+}$ concentration required for activity at low porphyrin concentration. Gun4 therefore controls magnesium chelatase at physiologically significant $Mg^{2+}$ concentrations and likely acts as a molecular switch in vivo so that in its absence magnesium chelatase is inactive. This mechanism could allow Gun4 to mediate magnesium protoporphyrin levels both for chlorophyll biosynthesis and for signaling to the nucleus.

Efficient production of light-harvesting complexes in plants and chlorophyll-synthesizing bacteria requires coordination between chlorophyll biosynthesis in the chloroplast and expression of genes for light-harvesting proteins in the nucleus. Uncoupling of these processes is deleterious, in part because an excess of chlorophyll or its precursors promotes photooxidative damage. Communication pathways from the chloroplast to the nucleus have been revealed through mutations in *Arabidopsis* that display a *g*enome *un*coupled (GUN) phenotype (*1*). Four of the genes identified as *gun* mutants (*gun2*−*5*) encode proteins that function in tetrapyrrole biosynthesis. They are heme oxygenase (*gun2*) and biliverdin reductase (*gun3*) from the heme catabolic pathway, and the porphyrin binding subunit of magnesium chelatase (*2*) (*gun5*) and a recently discovered protein (*gun4*) from the chlorophyll biosynthetic pathway (*3*, *4*).

Signaling through the pathway that is disrupted in *gun2*−*5* mutants is mediated by the chlorophyll biosynthetic inter-

[†] This work was supported by the BBSRC, U.K. (Grant 101670 to P.A.D. and C.N.H.), the NIH (Grant GM56775 to H.L.S. and C.P.H.), and the Offices of Biological and Environmental Research and of Basic Energy Sciences of the U.S. Department of Energy/National Center for Research Resources of the NIH (to A.H.).

[‡] Coordinate and structure factors have been deposited in the Protein Data Bank, accession codes 1Z3X (Gun4) and 1Z3Y (Gun4-1).

* To whom correspondence should be addressed. H.L.S.: tel, 801-585-3919; e-mail, heidi@biochem.utah.edu. C.N.H.: tel, (0)114-222-4191; e-mail, c.n.hunter@sheffield.ac.uk.

[§] These two authors contributed equally to this work.

[||] University of Sheffield.

[⊥] University of Utah.

[#] Brookhaven National Laboratory.

10.1021/bi050240x CCC: $30.25 
Published on Web 05/03/2005

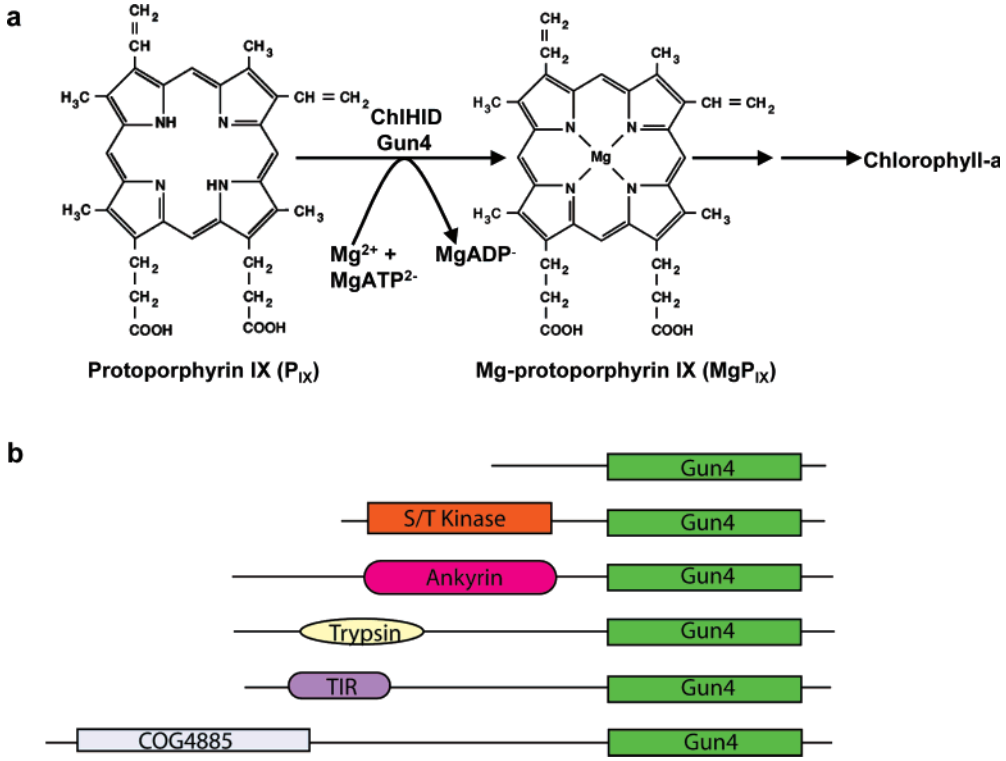


FIGURE 1: (a) Magnesium chelation step in chlorophyll biosynthesis. The chlorophyll biosynthetic pathway begins with the formation of $MgP_{IX}$ by the insertion of $Mg^{2+}$ into $P_{IX}$ catalyzed by magnesium chelatase, a multicomponent enzyme comprising H, I, and D subunits. The Gun4 protein is known to stimulate magnesium chelatase activity (*4*). (b) Structure of proteins that contain Gun4 domains. The Gun4 domain is found within the C-terminal region of a diverse range of proteins. Most of the homologues have an N-terminal extension of 70−120 residues that is highly divergent and lacks similarity to other characterized protein domains. Some proteins have recognizable domains; TIR is a toll−interleukin 1-resistance domain (function unknown); COG4885 is an uncharacterized domain conserved in archaea (function unknown).

mediate magnesium protoporphyrin IX ($MgP_{IX}$)[1] (*5*), which is produced by magnesium chelatase in the first committed step of the chlorophyll biosynthetic pathway (*6*, *7*) (Figure 1a). Magnesium chelatase is comprised of three protein subunits, ChlI (38−42 kDa), ChlD (60−74 kDa), and ChlH (*gun5*, 140−150 kDa) (BchIDH in photosynthetic bacteria) (*6*−*9*). ChlI is a $AAA^+$ ATPase (*10*, *11*) and contains a $Mg^{2+}$ binding site (*12*). ChlD forms a stable complex with ChlI (*10*) and is expected to adopt a similar ATPase structural fold, though the putative ATPase active site is incomplete and the protein does not catalyze ATP hydrolysis (*10*). The third subunit, ChlH, binds porphyrins (*2*, *13*) and presumably contains the active site for chelation.

Magnesium chelatase lies at a branch point in tetrapyrrole biosynthesis where insertion of $Mg^{2+}$ eventually results in the production of chlorophyll or the insertion of $Fe^{2+}$ produces heme. Consequently, magnesium chelatase is a prime candidate for pathway regulation (*2*, *17*, *18*) [for a recent comprehensive review see Grimm (*14*)] and is regulated in part by a cooperative response to magnesium (*15*). Free magnesium concentration is thermodynamically linked to chloroplast [ATP]:[ADP]:[$P_i$] status (*15*). In the dark, with $Mg^{2+}$ concentrations in the chloroplast approximately equal to ~0.5 mM (*16*), the chelatase will be essentially inactive, whereas in the daytime, when $Mg^{2+}$ concentrations rise, the chelatase is activated, permitting flux into the chlorophyll biosynthetic pathway. This cooperative response to free magnesium links photosynthetic ATP synthesis to the activity of the first enzyme in the pathway for photosynthetic pigment production (*15*). Other regulatory mechanisms operating on different time scales will undoubtedly exist, at the transcriptional level for example. It is known that the level of transcript for the porphyrin binding subunit of the chelatase, ChlH (*2*), oscillates significantly during a diurnal cycle (*17*), thereby obeying the imperatives of a circadian clock (*18*).

The activity of magnesium chelatase from higher plants and cyanobacteria is further enhanced by addition of the Gun4 protein (*4*). The mechanism of chelatase stimulation by Gun4 is not well understood, although clues are provided by the observations that Gun4 can bind the magnesium chelatase ChlH subunit as well as the porphyrin substrate and product of the chelatase reaction (*4*). Inactivation of the *gun4* gene in *Synechocystis* 6803 results in aberrant tetrapyrrole biosynthesis (*19*). *Arabidopsis* Gun4 is found in chloroplasts as part of a high molecular weight complex in thylakoid and the envelope membranes, as well as a soluble monomer in the stroma (*4*). Stimulation of magnesium chelatase activity affects the concentration of $MgP_{IX}$, the signaling molecule, and likely explains the importance of Gun4 for chloroplast to nucleus signaling.

To better understand the biochemical and mechanistic basis for Gun4 activity, we have determined the crystal structure of Gun4 from *Thermosynechococcus elongatus*, revealing a highly helical, two-domain protein. Surface-exposed residues that have been conserved throughout evolution cluster on the C-terminal domain, suggesting that this region functions

[1] Abbreviations: $P_{IX}$, protoporphyrin IX; $D_{IX}$, deuteroporphyrin IX; $MgP_{IX}$, magnesium protoporphyrin IX; $MgD_{IX}$, magnesium deuteroporphyrin IX; gun, genome uncoupled; GST, glutathione *S*-transferase.

Table 1: Crystallographic Data and Refinement

| | | | | |
|---|---|---|---|---|
| space group $P2_1$ | MAD peak | MAD inflection | MAD remote | gun4-1 |
| *a* (Å) | 58.3 | 58.3 | 58.4 | 58.3 |
| *b* (Å) | 40.7 | 40.7 | 40.7 | 40.7 |
| *c* (Å) | 62.4 | 62.4 | 62.4 | 61.9 |
| $\beta$ (deg) | 115.40 | 115.40 | 115.42 | 115.66 |
| $\lambda$ (Å) | 0.9796 | 0.9802 | 0.9660 | 1.54 |
| resolution (Å) (high)[a] | 50−1.5 (1.55−1.5) | 50−1.7 (1.76−1.7) | 50−1.75 (1.81−1.75) | 25−1.7 (1.76−1.70) |
| no. of total reflections | 911860 | 579868 | 581345 | 128124 |
| no. of unique reflections | 42482 | 29325 | 26640 | 28501 |
| completeness (%) | 99.9 (100) | 100 (100) | 100 (100) | 97.8 (80) |
| mosaicity (deg) | 0.72 | 0.6 | 0.5 | 0.68 |
| $I/\sigma(I)$ | 27 (5.3) | 41 (5.8) | 26 (7.3) | 30 (3.9) |
| $R_{merge}$[b] | 6.8 (46.7) | 7.9 (44.8) | 8.5 (44.6) | 3.9 (26.8) |
| refinement | | | | |
| $R_{cryst}$ (%)[c] | 17.9 | | | 18.0 |
| $R_{free}$ (%)[d] | 20.8 | | | 20.8 |
| protein residues modeled | −3 to 3, 6 to 235 | | | −3 to 3, 6 to 235 |
| no. of solvent molecules | 432 | | | 280 |
| RMSD bonds (Å) | 0.009 | | | 0.007 |
| RMSD angles (deg) | 1.163 | | | 1.019 |
| $\delta/\Psi$ angles | | | | |
| most favored (%) | 93.6 | | | 93.0 |
| additionally allowed (%) | 6.4 | | | 6.5 |
| $\langle B \rangle$ protein (Å$^2$) | 18.01 | | | 22.48 |
| $\langle B \rangle$ main chain (Å$^2$) | 17.28 | | | 21.93 |
| $\langle B \rangle$ water (Å$^2$) | 35.22 | | | 33.09 |

[a] Numbers in parentheses are for the high-resolution bin. [b] $R_{merge} = 100(\sum|I - \langle I \rangle|/\sum I)$, where $I$ is the intensity of an individual measurement and $\langle I \rangle$ is the average intensity from multiple observations. [c] $R_{cryst} = 100(\sum||F_o| - k|F_c||/\sum|F_o|)$. [d] $R_{free}$ equals the *R*-factor against 5% of the data removed prior to refinement.

to bind porphyrin and/or magnesium chelatase. This proposition was tested using a combination of site-directed mutagenesis and kinetic analysis. We find that Gun4 exerts a remarkable effect on magnesium chelatase by greatly increasing $V/K^{D_{IX}}$, the apparent first-order rate constant for interaction of porphyrin with the chelatase−nucleotide complex. At physiologically relevant $Mg^{2+}$ concentrations, Gun4 lowers the threshold $Mg^{2+}$ concentration required for activity at low, limiting porphyrin concentrations. Thus, Gun4 alters the $Mg^{2+}$ response of the chelatase, and in doing so it can alter the levels of the $MgP_{IX}$ product available for signaling and continued progress along the chlorophyll biosynthetic pathway.

## MATERIALS AND METHODS

*Protein Purification.* The full-length *Synechocystis* sp. PCC6803 and *T. elongatus* GUN4 genes were isolated by PCR from genomic DNA and expressed as glutathione *S*-transferase (GST) tag fusion proteins in *Escherichia coli* using pGEX-4-T1 (Amersham Biosciences). The fusion protein was purified on glutathione agarose 4 fast flow (Amersham) according to the manufacturer's specifications. The GST tag was cleaved by thrombin digestion and the thrombin removed using benzamidine Sepharose 4 fast flow (Amersham). For crystallization, the *T. elongatus* Gun4 was expressed as a GST fusion protein using the pGEX-4-T1 vector system and purified as for the *Synechocystis* protein. Following processing of the GST tag with thrombin the Gun4 was concentrated prior to loading onto an S75 size exclusion column (Pharmacia) equilibrated with 20 mM Tris, pH 8.5, 100 mM NaCl, and 1 mM DTT. Gun4 eluted from the column at a volume consistent with a monomeric form of the protein and was concentrated to 7 mg/mL prior to crystallization. Selenomethionine incorporation was achieved using the methionine inhibition method (*28*) and was purified and crystallized in the same conditions as wild-type protein. The expression vectors pET9a-ChlI, pET9a-$His_6$ChlD, and pET9a-$His_6$ChlH were used to produce recombinant magnesium chelatase subunits essentially as described previously (*7*, *10*).

*Mutagenesis.* The *Synechocystis* Gun4-1 and several *T. elongatus* mutants were generated in pGEX-4-T1 using the QuikChange mutagenesis kit (Stratagene) and expressed and purified as above.

*Crystallization and Structure Determination. T. elongatus* Gun4 was crystallized by sitting drop vapor diffusion methods using 2 $\mu$L of protein mixed with 2 $\mu$L of a well solution consisting of 20% PEG 3350 and 0.2 M $NH_3Cl$ at 4 °C. Crystals grew in the form of flat plates and were cryoprotected by transfer to a solution of the well conditions made up with 25% glycerol. The crystals belong to space group $P2_1$. MAD data were collected around the selenium peak edge at Brookhaven National Laboratory. Data for the Gun4-1 mutant were collected using a Rigaku rotating anode and a RAXIS IV detector. All data were processed and scaled using the HKL package (*29*) (Table 1). Two selenium sites were identified and protein phases calculated using SOLVE (*30*) followed by solvent flattening (45% solvent) using RESOLVE (*31*). The program RESOLVE autotraced a preliminary model, including correct side chains, for 200 of the final 235 residues. The model was refined against all data to 1.5 Å resolution using REFMAC (*32*), within the CCP4 suite of proteins (*33*) (Table 2).

*Porphyrin Binding.* Porphyrin binding was detected using Trp quenching as described previously (*2*).

*Chelatase Assays.* Assay conditions and detection systems were essentially as described previously (*24*). Purified magnesium chelatase subunits were used, and reactions were run at 34 °C, $I = 0.1$, and pH 7.7 in 50 mM MOPS/KOH, 0.3 M glycerol, and 1 mM DTT. Assays were initiated by

Table 2: Dissociation Constants ($K_d$) of Several Purified Wild-Type and Mutant Gun4 Proteins from *Synechocystis* and *T. elongatus* for Deuteroporphyrin IX ($D_{IX}$) and Magnesium Deuteroporphyrin IX ($MgD_{IX}$) As Determined by Tryptophan Fluorescence Quenching

| species | protein | $D_{IX}$ $K_d$ ($\mu$M) | $MgD_{IX}$ $K_d$ ($\mu$M) |
|---|---|---|---|
| *Synechocystis* | Gun4 | $2.29 \pm 0.28$ | $0.30 \pm 0.02$ |
| | Gun4-1 | $0.15 \pm 0.06$ | $0.04 \pm 0.02$ |
| *T. elongatus* | Gun4 | $1.73 \pm 0.19$ | $0.24 \pm 0.06$ |
| | Gun4-1 | $0.16 \pm 0.02$ | $0.04 \pm 0.01$ |
| | N216A | $2.64 \pm 0.19$ | $1.68 \pm 0.30$ |
| | R219A | $2.29 \pm 0.10$ | $2.18 \pm 0.06$ |
| | Y197A | $10.26 \pm 2.28$ | $4.24 \pm 0.71$ |

addition of enzyme to give a final concentration of 0.2 $\mu$M ChlI, 0.1 $\mu$M $His_6$ChlD, and 0.4 $\mu$M $His_6$ChlH. This subunit ratio was previously shown to give an optimal enzyme activity (*24*). Production of $MgD_{IX}$ was monitored by increase in fluorescence in 100 $\mu$L reactions, recorded using a Bio-Tek F2 microplate reader with excitation through a $420 \pm 25$ nm filter and emission observed through a $590 \pm 17.5$ nm filter (*2*, *23*). Steady-state rates were estimated from chelation progress curves using the instrument software. At a fixed free $Mg^{2+}$ concentration apparent kinetic parameters for the other two substrates ($V^{app}$, $V/K^{MgATP(app)}$, $V/K^{D_{IX}(app)}$, $V/K^{MgATP:D_{IX}(app)}$) were estimated from hyperbolic fits to primary and secondary plots as described previously (*15*). Nonlinear regression analysis was performed using Sigmaplot 8.0 (SPSS).

## RESULTS

*Gun4 Domain Sequences.* We searched for related proteins by submitting the *Arabidopsis thaliana* Gun4 sequence to a BLASTP (*20*) search and inspection of the 50 highest scoring sequences. These homologues, which derive from photosynthetic organisms from cyanobacteria to maize, all contain a single copy of a domain of ~150 amino acid residues that shares at least 28% sequence identity with *Arabidopsis* Gun4. This Gun4 domain has been characterized by several database analyses: domain PD013515 identified by ProDom (*21*) and domain 05419 by pfam (*22*). Most of the homologues contain the Gun4 domain at their C-terminus and have an N-terminal extension of 70−120 residues that is highly divergent and lacks similarity to other characterized protein domains. In many cases these N-terminal sequences have high predicted helical propensity, although the *Arabidopsis* and rice sequences are predicted to contain loops and strands in this region. Several cyanobacterial sequences have longer N-terminal regions that contain another recognizable functional domain, such as kinase, protease, and putative protein binding domains (Figure 1b). The presence of Gun4 domains within larger molecules suggests that they might function in other contexts to perform additional roles in signaling or regulation.

*Structure Determination.* We were able to grow crystals of the purified, recombinant Gun4 protein from *T. elongatus.* This homologue and the Gun4 protein identified in *Arabidopsis* share 41% sequence identity in their C-terminal Gun4 domains and have N-terminal extensions of similar length containing no significant sequence similarity. The *T. elongatus* and *Synechocystis* Gun4 proteins used in our structural and biochemical experiments belong to the Gun4 family subgroup possessing a helical N-terminal domain. The widely differing conservation of the N- and C-terminal domains is nicely illustrated by these two proteins; the N-terminal regions show no recognizable sequence identity whereas the C-terminal Gun4 domains share 57% sequence identity.

The crystal structure of *T. elongatus* Gun4 was determined by MAD phasing using data collected from a crystal of selenomethionine-substituted protein and refined against 1.5 Å data to $R_{cryst}/R_{free}$ values of 17.9%/20.8% (Table 1). The model includes three residues of the six additional N-terminal residues remaining following the removal of the GST tag (−3 through −1) and all residues of the coding sequence except residues 4 and 5, which are disordered. The average *B*-factor of the structure is 16.1 Å$^2$, and all residues lie in allowed regions of the Ramachandran plot.

*Structure Description.* As anticipated from the sequence, the *T. elongatus* Gun4 structure reveals two distinct, almost entirely helical, domains (Figure 2a). The N-terminal domain contains five helices arranged in an alternating antiparallel pattern that resembles ARM or HEAT repeats. Proteins with these motifs often function in protein−protein interactions, although the functional importance of this poorly conserved domain in Gun4 is currently unknown. Helices are named HA−HE in the N-terminal domain and H1−H8 in the C-terminal domain. The N- and C-terminal domains are connected by an extended loop between the HE and H1 helices (residues 83−98). The two domains share ~600 Å$^2$ surface area at their interface, suggesting that the conformation observed in the crystal is likely to be maintained in solution.

The highly conserved Gun4 domain consists of eight helices organized as a globular bundle with no significant resemblance to known structures in the protein databank. The first half of the C-terminal domain is formed by a three-helix bundle (H1, H2, and H5), with the small H3 and H4 helices packing at the bottom of structure (Figure 2a). The second half of the C-terminal domain is comprised of three additional helices (H6, H7, and H8) and a small C-terminal helical turn. All of the loops connecting the helices are short (maximum of six residues), except for the loop between N- and C-terminal domains (above) and a long unstructured loop (36 residues) between H7 and H8 (Figure 2a, colored in red).

*Gun4-1 Structure.* To investigate the structural basis for the Gun4-1 mutation in *Arabidopsis*, which gives rise to chlorophyll deficiency and a consequent disruption of chloroplast to nucleus signaling (*4*), we constructed the Gun4-1 mutant equivalents *Synechocystis* Leu100Phe and *T. elongatus* Leu105Phe. We refer to these mutants as the Gun4-1 proteins. In the *T. elongatus* structure Leu105 is located in helix H1 and projects into a hydrophobic region between helices H2 and H4 (Figures 2a and 3b). We grew crystals for the *T. elongatus* Gun4-1 protein and collected data to 1.7 Å. The structure was solved by molecular replacement and refined to $R_{cryst}/R_{free}$ values of 18%/20.8% (Table 1). The crystal structures of wild-type Gun4 and Gun4-1 superimpose with an RMSD of just 0.24 Å over all Cα atoms (Figure 2b). Neither Leu105 of the wild-type protein nor the Phe105 of Gun4-1 displays any atoms at the protein surface. The surface features of the two proteins are essentially identical. This indicates that the phenotypic consequences of the gun4-1 mutations do not result from alterations in the structure.

*Protoporphyrin IX Binding Site.* All of the residues that are invariant in the sequence alignment shown in Figure 2c

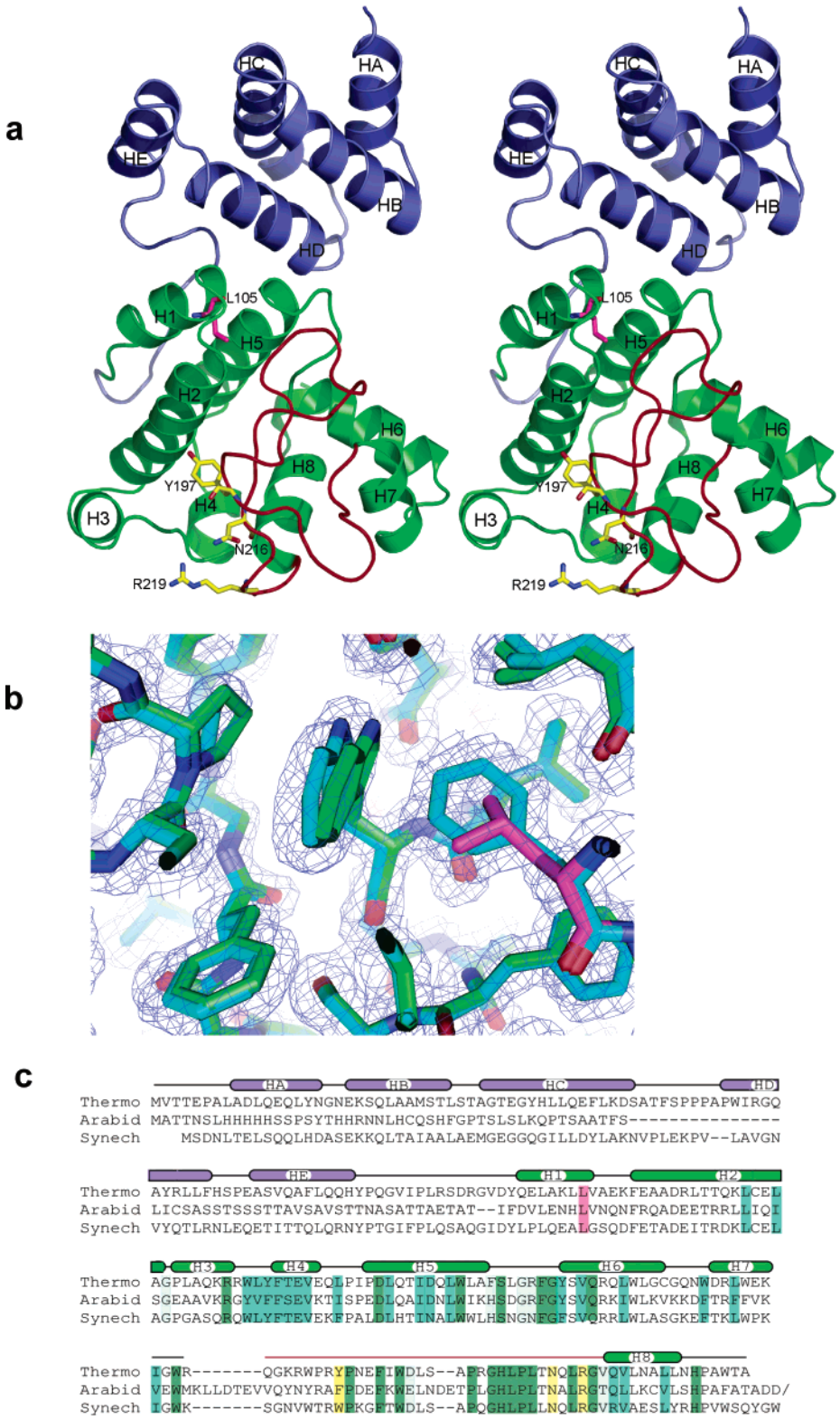


FIGURE 2: (a) Structure of *T. elongatus* Gun4 depicted in stereo. Two helical domains are present, an N-terminal nonconserved domain (blue in panel A) and the conserved Gun4 domain (green). A long loop lacking regular secondary structure contains many invariant residues and may play a role in ligand binding (red). Leu105, which is changed to Phe in the Gun4-1 mutant, is colored magenta. Residues changed to Ala for biochemical studies reported in this paper are shown in yellow: Tyr197, Asn216, and Arg219. (b) Superposition of the wild-type (green) and Gun4-1 (cyan: Leu105Phe) structures with the wild-type leucine residue in magenta. The $2F_o - F_c$ electron density (blue, 2.0 Å resolution displayed at 1$\sigma$) is for the Gun4-1 mutant. (c) Sequence alignment of Gun4 proteins shown with the secondary structure of *T. elongatus* Gun4 color-coded as in panel a. Three sequences are shown, which are Gun4 from *T. elongatus*, *A. thaliana*, and *Synechocystis* PCC6803. The alignment is color-coded by conservation based on a larger alignment available as a Supporting Information Figure S1. Invariant residues are in dark green and less conserved residues in lighter shades of green. The Leu105 position, which is changed to Phe in the Gun4-1 mutant, is highlighted in magenta, and the three highly conserved residues that were mutated in this study are highlighted in yellow.

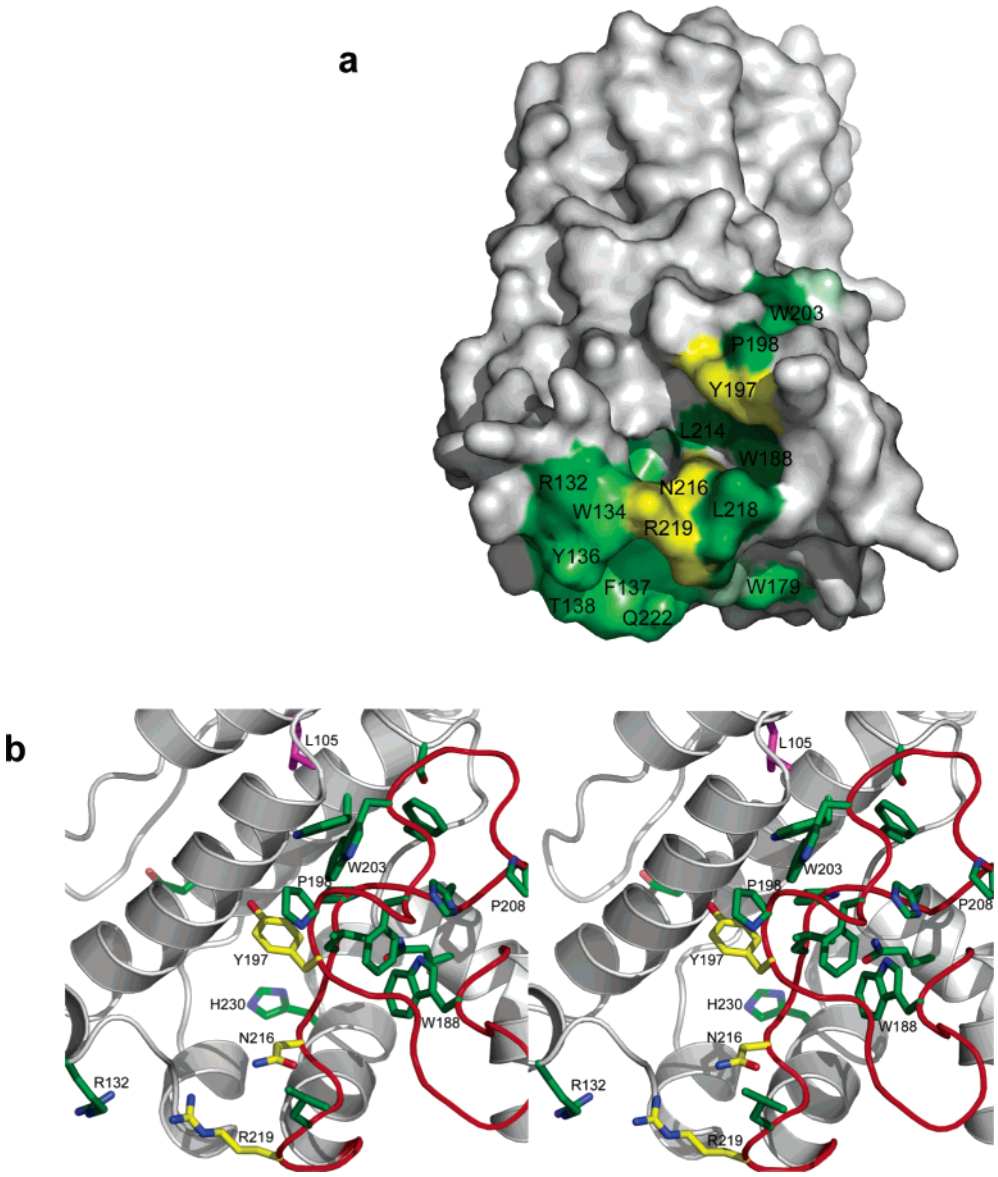


FIGURE 3: Protoporphyin binding site. (a) Solvent-accessible surface of Gun4 colored by conservation as seen in Figure 2c. (b) Close-up stereoview of the probable binding site.

(see Supporting Information Figure S1 for an alignment of 12 diverse sequences), and are also surface exposed in the *T. elongatus* Gun4 crystal structure, are found on the 36-residue loop between H7 and H8 or on spatially adjacent regions of the C-terminal Gun4 domain (Figure 2a). Some 15 invariant and exposed side chains form an extensive patch on the Gun4 surface (Figure 3). A cleft is located in the midst of these conserved surface residues that is approximately 10 Å by 12 Å wide and 8−10 Å deep, with two deeper indentations into the core of the protein separated by a ridge formed by Leu214 and Asn216 (Figure 3a). Residues surrounding this cleft include the conserved side chains of Arg132, Leu218, Tyr197, and Arg219 (see Supporting Information Figure S1), while inside the cleft the conserved residues Trp188, Leu214, and Asn216 are solvent accessible (Figure 3).

Initial studies suggested that Gun4 binds porphyrin ligands and that this binding may be responsible for Gun4's role in cellular signaling (*4*). Simple modeling indicates that the cleft described above can accommodate approximately half of a protoporphyrin IX molecule, with the propionate side chains solvent accessible and projecting toward the conserved arginine side chains (Arg132 and Arg219). An interaction of this nature might be sufficient to specifically recognize the porphyrin ligand. It also appears possible that minor conformational changes might greatly increase the size of the cleft in order to accommodate a more extensive interaction. For example, the Arg219 side chain is likely to be flexible in solution, and displacement from its crystallographically observed position would significantly enlarge the cleft toward the bottom of the structure (viewed from Figure 2a).

*Porphyrin Binding.* To test the hypothesis that the cleft is the porphyrin binding site, the binding affinity of porphyrin substrate and product for the wild-type and mutant Gun4 proteins was determined. Three mutants, Tyr197Ala, Asn216Ala, and Arg219Ala, were constructed because these residues are part of the cleft (Figure 3a). Porphyrin binding constants were estimated from changes in the intrinsic fluorescence of Gun4 protein provoked by binding of a water-soluble protoporphyrin mimic, deuteroporphyrin ($D_{IX}$) (Figure 4 and Table 2), using methodology already estab-

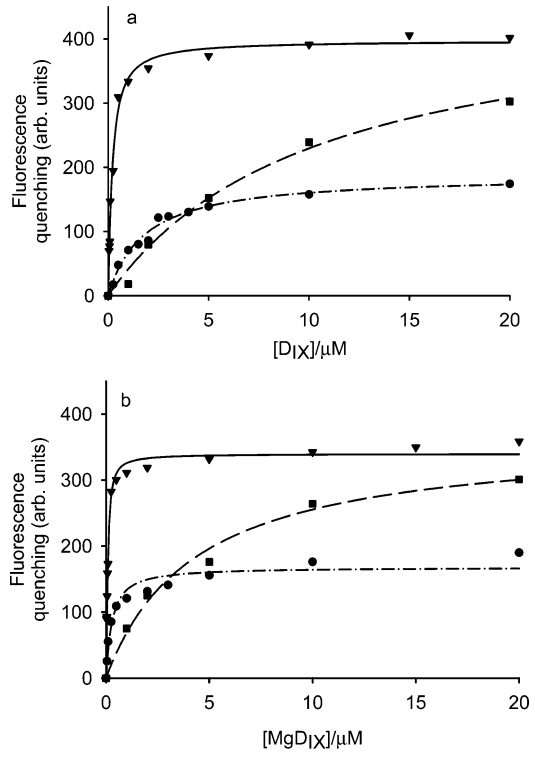


FIGURE 4: Porphyrin binding studies of wild-type and mutant Gun4 proteins from *T. elongatus*. Each graph depicts the quenching of Gun4 fluorescence by increasing levels of either (a) deuteroporphyrin ($D_{IX}$) or (b) magnesium deuteroporphyrin ($MgD_{IX}$). The proteins used were *T. elongatus* wild-type Gun4 (dot and dashed line), Gun4-1 (solid line), and mutant Y197A (dashed line).

lished for porphyrin binding to the magnesium chelatase H subunit (*2*). Analyses were performed on both the *T. elongatus* and *Synechocystis* Gun4 proteins since the structural data stem from the former organism, and most previously published kinetic analyses for magnesium chelatase were performed using proteins from the latter organism (*2*, *12*, *15*, *23*, *24*). The Gun4-1 mutations were also analyzed to investigate if the Gun4-1 phenotype stems from a kinetic malfunction.

All proteins tested displayed a tighter binding affinity to $MgD_{IX}$ than $D_{IX}$. This suggests that the protein specifically selects for ligand containing the central metal ion. *T. elongatus* Gun4 binds $MgD_{IX}$ significantly more strongly than it binds $D_{IX}$ (Figure 4a, b), with $K_d$ values of $0.24 \pm 0.06$ and $1.73 \pm 0.19$ $\mu$M, respectively. A similar pattern of binding was observed for the *Synechocystis* Gun4 (Table 2 and Supporting Information Figure S2), consistent with the results obtained by Larkin and co-workers (*4*).

Surprisingly, the Gun4-1 mutants display significantly increased affinity for both $D_{IX}$ and $MgD_{IX}$ (Figure 4 and Table 2), with the $K_d$ for $D_{IX}$ decreased 15-fold and 11-fold for the *Synechocystis* and *T. elongatus* proteins, respectively. The effect on $MgD_{IX}$ binding was slightly less pronounced, but nevertheless the Gun4-1 mutation increased the binding affinity for $MgD_{IX}$ by 8-fold and 6-fold, respectively, for the *Synechocystis* and *T. elongatus* proteins. The structural basis of these findings and their functional implications are unclear.

The fluorescence quenching data support the proposal that binding of porphyrin ligands involves the cluster of conserved residues defined in part by Tyr197, Asn216, and Arg219. In particular, the binding affinity of Y197A Gun4 for $MgD_{IX}$ is reduced ~18-fold compared to the wild type (Figure 4b and Table 2), and the affinity for $D_{IX}$ was reduced 6-fold (Figure 4a and Table 2). Mutation of Asn216 and Arg219 to Ala also weakened ligand binding (7−8-fold), but in these cases the effect was specific for $MgD_{IX}$ (Table 2 and Supporting Information Figure S2).

*Gun4 and Magnesium Chelatase Activity.* To further understand the functional basis for Gun4 stimulation of magnesium chelatase activity, we have studied the wild-type and mutant Gun4 proteins by steady-state kinetic analysis. As already demonstrated (*4*), purified *Synechocystis* Gun4 stimulates the activity of the cognate magnesium chelatase formed from subunits ChlI, ChlD, and ChlH. Fortuitously, we were also able to examine Gun4 proteins from *T. elongatus* in a heterologous assay system employing the *Synechocystis* ChlI, ChlD, and ChlH magnesium chelatase subunits. Gun4-1 mutants from both species as well as the *T. elongatus* point mutants impaired in porphyrin binding were also studied.

Titration of Gun4 protein into steady-state magnesium chelatase reactions in which porphyrin substrate is saturating allows two important aspects of Gun4 stimulation to emerge, namely, the extent of activation at maximal Gun4 concentrations and the strength of interaction of Gun4 with the chelatase (Figure 5). A plot of the rate of Mg chelation at saturating concentrations of $D_{IX}$ (8 $\mu$M) (open circles in Figure 5) with increasing concentrations of *Synechocystis* Gun4 is characterized by a hyperbolic curve where the steady-state chelation rate increases approximately 2-fold (Figure 5a). The maximum increase in steady-state rate is reached when Gun4 concentrations approximately equal that of the catalytic subunit, ChlH (Figure 5a). Figure 5c shows that the *T. elongatus* Gun4 is also able to activate the maximum steady-state rate of *Synechocystis* magnesium chelatase, but it requires a higher concentration of *T. elongatus* Gun4 to achieve this effect, indicating a weaker interaction with the *Synechocystis* chelatase. The *Synechocystis* and *T. elongatus* Gun4-1 mutants mirror the behavior of the wild-type proteins and are not at all disrupted in their ability to stimulate magnesium chelatase (Figure 5b,d, open circles). The mutant *T. elongatus* Gun4 proteins (Y197A, N216A, and R219A) that are impaired in porphyrin binding also stimulate *Synechocystis* chelatase activity to a similar extent as wild type (Figure 5e; see Supporting Information Figure S3 for N216A and R219A), indicating that there appears to be no link between porphyrin binding capacity and stimulation of enzyme activity under saturating porphyrin conditions.

These initial studies were carried out at saturating substrate concentrations, levels that may mask the porphyrin binding deficiencies of the *T. elongatus* point mutants. Additional studies were therefore carried out at lower, more physiological concentrations of $D_{IX}$ (0.8 $\mu$M) (Figure 5, solid circles). Figure 5a shows that, at limiting porphyrin concentrations, *Synechocystis* Gun 4 exerts a significantly greater effect on magnesium chelatase, with an approximately 6-fold stimulation, compared with 2-fold stimulation at 8 $\mu$M porphyrin (Figure 5a, open circles). The Gun4-1 mutation does not affect this stimulation. Similar data are obtained with the *T. elongatus* Gun4 and Gun4-1 proteins (Figure 5c,d, solid circles), and it appears that a slightly tighter interaction with

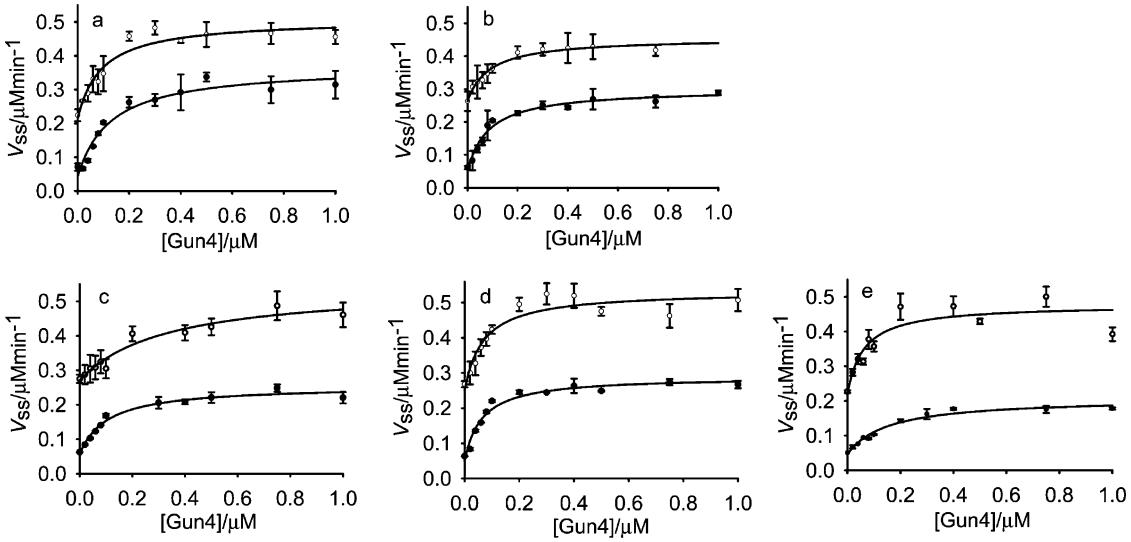


FIGURE 5: Titration of *Synechocystis* magnesium chelatase activity with Gun4. The open circles correspond to experiments conducted with saturating levels of $D_{IX}$ (8 $\mu$M $D_{IX}$; 5 mM $MgATP^{2-}$, and 15 mM $Mg^{2+}$); the solid circles correspond to a limiting $D_{IX}$ concentration (0.8 $\mu$M $D_{IX}$; 5 mM $MgATP^{2-}$, and 15 mM $Mg^{2+}$). Experiments were performed in duplicate; each point is the mean value with the range of error. In all cases the magnesium chelatase is formed from the *Synechocystis* H, I, and D subunits. (a) Titration with *Synechocystis* Gun4; (b) titration with the *Synechocystis* Gun4-1 mutant protein; (c) *T. elongatus* Gun4; (d) *T. elongatus* Gun4-1; (e) *T. elongatus* Y197A.

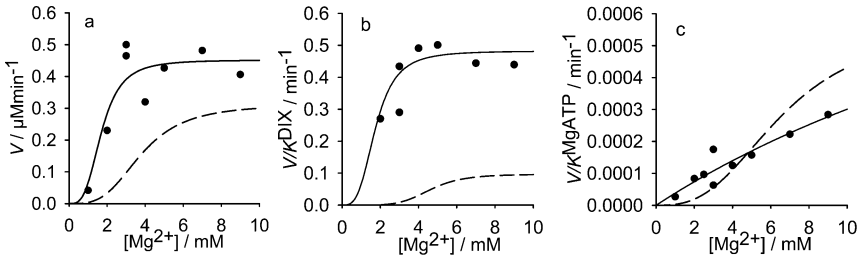


FIGURE 6: $Mg^{2+}$ dependence of the $MgATP^{2-}$ and $D_{IX}$ apparent kinetic parameters for the *Synechocystis* magnesium chelatase. The data obtained in the presence of a near-saturating concentration (0.25 $\mu$M) of Gun4 (solid lines) were fitted to either the Hill equation (a, b) or the Michaelis−Menten equation (c) and can be compared qualitatively to fitted (dashed) lines previously obtained in the absence of Gun4 (*15*). (A) $V^{app}$ versus [$Mg^{2+}$]; (B) $V/K^{D_{IX}(app)}$ versus [$Mg^{2+}$]; saturating $MgATP^{2-}$; (C) $V/K^{MgATP(app)}$ versus [$Mg^{2+}$]; saturating $D_{IX}$.

the chelatase occurs when testing the *T. elongatus* Gun4-1, as noted previously during saturating porphyrin conditions (Figure 5d). Of the site-directed mutants, N216A and R219A are unaffected, but Y197A, with the most impaired porphyrin binding, has suffered a loss in activity, with a reduction of approximately 25% in its ability to stimulate magnesium chelatase at saturating Gun4 levels (Figure 5e).

*Mg Cooperativity.* To determine the mechanistic basis for the acceleration of the magnesium chelatase reaction by Gun4, additional steady-state kinetic analysis was undertaken. We have previously demonstrated that in the absence of Gun4 the *Synechocystis* enzyme exhibits positive cooperativity to $Mg^{2+}$ in the physiologically relevant range between 1 and 8 mM (*15*). We therefore explored the steady-state behavior of magnesium chelatase in the presence of saturating concentrations of Gun4 to examine whether Gun4 exerts an influence on the $Mg^{2+}$ regulation of the enzyme.

Gun4 dramatically enhances the sensitivity of magnesium chelatase to $Mg^{2+}$ concentrations. In the presence of near-saturating Gun4, positive cooperativity with respect to $Mg^{2+}$ is retained, stimulating the maximum rate, $V$, by ~40% from 0.31 to 0.43 ± 0.03 $\mu$M/min (Figure 6a). Furthermore, the specificity constant for $D_{IX}$, $V/K^{D_{IX}}$, is increased 5-fold from 0.097 to 0.47 ± 0.05 $min^{-1}$ at saturating $Mg^{2+}$ and $MgATP^{2-}$ (Figure 6b), demonstrating that Gun4 increases the efficiency of the chelatase.

The true significance of Gun4 appears to be revealed at low $Mg^{2+}$ concentrations, where a dramatic enhancement of $V/K^{D_{IX}}$ occurs such that at 2 mM $Mg^{2+}$ magnesium chelatase is virtually inactive in the absence of Gun4 but essentially fully active in its presence. Little effect on $Mg^{2+}$ cooperativity is exerted by Gun4 under conditions where $D_{IX}$ is saturating (Figure 6c). This behavior is likely to be physiologically significant as it is already known that $Mg^{2+}$ levels in the plastid fluctuate within this range of concentrations (*16*).

## DISCUSSION

The physiological importance of Gun4 in regulating $MgP_{IX}$ levels and in coupling plastid metabolism to nuclear gene expression has prompted a comprehensive assessment of Gun4 stimulation of magnesium chelatase. The highly helical Gun4 protein contains an unstructured region harboring many evolutionary invariant residues and forms part of a cleft on the surface of the protein that may contain the porphyrin binding site. Binding measurements showed that both the *T. elongatus* and *Synechocystis* Gun4 proteins display a marked preference for $MgD_{IX}$ relative to $D_{IX}$ and that residues Tyr197, Asn216, and Arg219 are involved in ligand recognition (*3*). This selectivity for $MgD_{IX}$ rather than $D_{IX}$ is consistent with a role for Gun4 in regulating $MgP_{IX}$ levels.

It might have been expected that the Gun4-1 mutation, responsible in *Arabidopsis* for a signaling-deficient phenotype (*4*), would arise from impaired biochemical activity. Instead, we found that both the *T. elongatus* and *Synechocystis* Gun4-1 mutants had acquired enhanced porphyrin binding properties, by up to 15-fold, while maintaining the differential response to $MgD_{IX}$, relative to $D_{IX}$, seen for the wild-type Gun4. This tighter binding was not accompanied by loss of function, in terms of stimulation of the steady-state rate of chelation at saturating concentrations of porphyrin. Nor is this stimulation affected at subsaturating levels of porphyrin, which is arguably a more realistic mimic of in vivo conditions. Indeed, there seems to be no direct relationship between selective binding of $MgD_{IX}$ by Gun4 and stimulation of magnesium chelatase.

A detailed kinetic analysis of the influence of Gun4 on the chelatase reaction shows that Gun4 primarily acts to increase $V/K^{D_{IX}}$, the specificity constant for porphyrin, particularly at low magnesium concentrations. This is the apparent first-order rate constant for (limiting) porphyrin reacting with an enzyme−nucleotide complex, and it is the kinetic parameter that reflects the overall efficiency of transformation of the porphyrin substrate to metalloporphyrin product. Thus, Gun4 exerts a powerful effect on magnesium chelatase, measured as $V/K^{DIX}$, by reducing the $Mg^{2+}$ concentration required for activity. These effects are likely to be physiologically significant as the in vivo $Mg^{2+}$ concentration varies in the 0.5−6 mM range in response to ATP synthesis and consumption (*16*). From the point of view of catalysis and biosynthesis, therefore, Gun4 participates in the regulation of magnesium chelatase by matching the turnover of the first committed enzyme in the chlorophyll biosynthetic pathway to the prevailing $Mg^{2+}$ and $MgATP^{2-}$ concentrations.

It is clear from our titration data that lowered levels of active Gun4 protein will significantly reduce the production of $MgP_{IX}$ by magnesium chelatase and ultimately decrease chlorophyll levels. This will be exacerbated when $P_{IX}$ is limiting. The complete absence of Gun4 can shut down chelatase activity almost completely, as seen in Figure 6. Although one should be cautious about extrapolating from cyanobacteria to the situation in higher plants, this is consistent with the suggestion that the signaling defect of the Gun4-1 protein (*4*) results from low in vivo levels. Similarly, the in vivo counterpart to a complete absence of Gun4 was seen with the null allele *gun4-2*, which displayed severely impaired growth (*4*). It is clear that flux through magnesium chelatase, which occupies such an important biosynthetic role in cyanobacteria and plants, is stringently controlled and that Gun4 is essential to maintain a balanced flow along the chlorophyll biosynthetic pathway. Gun4 has a pivotal role at the branch point of tetrapyrrole biosynthesis in *Synechocystis*; its function is apparently not confined to optimizing magnesium chelatase activity as shown by the fact that *Synechocystis* will not tolerate complete abolition of Gun4 (*19*). Cyanobacteria have a dominant $Fe^{2+}$ branch of tetrapyrrole biosynthesis and *gun4* mutants also show decreased ferrochelatase, as well as reduced magnesium chelatase and methyltransferase (the next enzyme in the pathway), activities (*19*). Two roles have been postulated for Gun4 in *Synechocystis*: optimization of $P_{IX}/MgP_{IX}$ distribution to both chelatases and the methyltransferase, and stabilization of both chelatases (*19*). In *Arabidopsis* reducing Gun4 activity and $MgP_{IX}$ production would also be expected to have an effect on signaling, and the greatly enhanced affinity for $MgP_{IX}$ exhibited by Gun4-1 is likely to exacerbate the problem, by reducing the level of "free" $MgP_{IX}$ even further. How Gun4 exerts its control on both tetrapyrrole synthesis and signaling, either through activation of magnesium/iron chelatase activity and/or chanelling of $MgP_{IX}$, is a matter that requires further investigation.

This view of Gun4 focuses on its role as a component of chlorophyll biosynthesis, rather than on an explicit function as a signaling protein. In this regard, it should be noted that another *gun* mutation, *gun5* (*3*), results from a mutation in the magnesium chelatase H subunit, which also has a primary role in catalysis (*6*, *7*). Given that $MgP_{IX}$ is the substrate for the next enzyme in the pathway, the methyltransferase, the availability of this pigment for signaling functions might also involve close coupling between the chelatase and methyltransferase, such as that observed in a recombinant strain of *E. coli* harboring genes for both enzymes (*25*) and in transgenic tobacco plants with reduced and enhanced levels of the methyltransferase (*34*). A complete understanding of $MgP_{IX}$ availability for signaling will therefore require the study of steady-state and pre-steady-state kinetics of the methyltransferase (*25*, *26*).

## ACKNOWLEDGMENT

We thank Joanne Viney and Samantha Bailey for technical assistance. Data for this study were measured at beamline X26C of the National Synchrotron Light Source.

## SUPPORTING INFORMATION AVAILABLE

Protein alignment of Gun4 proteins from 12 different species, porphyrin binding studies of wild-type and mutant Gun4 proteins from *Synechocystis* and site-directed mutants of *T. elongatus* (N216A and R219A), and titration of magnesium chelatase activity of two site-directed mutants of *T. elongatus* (N216A and R219A) with Gun4. This material is available free of charge via the Internet at http://pubs.acs.org.

## REFERENCES

1. Susek, R. E., Ausubel, F. M., and Chory, J. (1993) Signal transduction mutants of *Arabidopsis* uncouple nuclear CAB and RBCS gene expression from chloroplast development, *Cell 74*, 787−799.
2. Karger, G. A., Reid, J. D., and Hunter, C. N. (2001) Characterization of the binding of deuteroporphyrin IX to the magnesium chelatase H subunit and spectroscopic properties of the complex, *Biochemistry 40*, 9291−9299.
3. Mochizuki, N., Brusslan, J. A., Larkin, R., Nagatani, A., and Chory, J. (2001) *Arabidopsis* genomes uncoupled 5 (GUN5) mutant reveals the involvement of Mg-chelatase H subunit in plastid-to-nucleus signal transduction, *Proc. Natl. Acad. Sci. U.S.A. 98*, 2053−2058.
4. Larkin, R. M., Alonso, J. M., Ecker, J. R., and Chory, J. (2003) GUN4, a regulator of chlorophyll synthesis and intracellular signaling, *Science 299*, 902−906.
5. Kropat, J., Oster, U., Rudiger, W., and Beck, C. F. (1997) Chlorophyll precursors are signals of chloroplast origin involved in light induction of nuclear heat-shock genes, *Proc. Natl. Acad. Sci U.S.A. 94*, 14168−14172.
6. Gibson, L. C. D., Willows, R. D., Kannangara, C. G., von Wettstein, D., and Hunter, C. N. (1995) Magnesium-protoporphyrin chelatase of *Rhodobacter sphaeroides*: reconstitiution of

activity by combining the products of the *bchH*, *-I* and *-D* genes expressed in *Escherichia coli*, *Proc. Natl. Acad. Sci. U.S.A. 92*, 1941−1944.
7. Jensen, P. E., Gibson, L. C. D., Henningsen, K. W., and Hunter, C. N. (1996) Expression of the *chlI*, *chlD*, and *chlH* genes from the cyanobacterium *Synechocystis* PCC6803 in *Escherichia coli* and demonstration that the three cognate proteins are required for magnesium-protoporphyrin chelatase activity, *J. Biol. Chem. 271*, 16662−16667.
8. Jensen, P. E., Willows, R. D., Petersen, B. L., Vothknecht, U. C., Stummann, B. M., Kannangara, C. G., von Wettstein, D., and Henningsen, K. W. (1996) Structural genes for Mg-chelatase subunits in barley: *Xantha-f*, *-g* and *-h*, *Mol. Gen. Genet. 250*, 383−394.
9. Papenbrock, J., Gräfe, S., Kruse, E., Hänel, F., and Grimm, B. (1997) Mg-chelatase of tobacco: identification of a *Chl D* cDNA sequence encoding a third subunit, analysis of the interaction of the three subunits with the yeast two-hybrid system, and reconstitution of the enzyme activity by co-expression of recombinant CHL D, CHL H and CHL I, *Plant J. 12*, 981−990.
10. Jensen, P. E., Gibson, L. C. D., and Hunter, C. N. (1998) Determinants of catalytic activity with the use of purified I, D and H subunits of the magnesium protoporphyrin IX chelatase from *Synechocystis* sp. PCC6803, *Biochem. J. 334* (Part 2), 335−344.
11. Fodje, M. N., Hansson, A., Hansson, M., Olsen, J. G., Gough, S., Willows, R. D., and Al Karadaghi, S. (2001) Interplay between an AAA module and an integrin I domain may regulate the function of magnesium chelatase, *J. Mol. Biol. 311*, 111−122.
12. Reid, J. D., Siebert, C. A., Bullough, P. A., and Hunter, C. N. (2003) The ATPase activity of the ChlI subunit of magnesium chelatase and formation of a heptameric AAA+ ring, *Biochemistry 42*, 6912−6920.
13. Willows, R. D., and Beale, S. I. (1998) Heterologous expression of the *Rhodobacter capsulatus* BchI, *-D*, and *-H* genes that encode magnesium chelatase subunits and characterization of the reconstituted enzyme, *J. Biol. Chem. 273*, 34206−34213.
14. Grimm, B. (2003) Regulatory Mechanisms of Eukaryotic Tetrapyrrole Biosynthesis, in *The Porphyrin Handbook* (Kadish, K. M., Smith, K. M., and Guilard, R., Eds.) Vol. 12, pp 1−32, Elsevier, New York.
15. Reid, J. D., and Hunter, C. N. (2004) Magnesium-dependent ATPase activity and cooperativity of magnesium chelatase from *Synechocystis* sp. PCC6803, *J. Biol. Chem. 279*, 26893−26899.
16. Ishijima, S., Uchibori, A., Takagi, H., Maki, R., and Ohnishi, M. (2003) Light-induced increase in free $Mg^{2+}$ concentration in spinach chloroplasts: Measurement of free $Mg^{2+}$ by using a fluorescent probe and necessity of stromal alkalinization, *Arch. Biochem. Biophys. 412*, 126−132.
17. Gibson, L. C. D., Marrison, J. L., Leech, R. M., Jensen, P. E., Bassham, D. C., Gibson, M., and Hunter, C. N. (1996) A putative Mg chelatase subunit from *Arabidopsis thaliana* cv C24. Sequence and transcript analysis of the gene, import of the protein into chloroplasts, and *in situ* localization of the transcript and protein, *Plant Physiol. 111*, 61−71.
18. Harmer, S. L., Hogenesch, J. B., Straume, M., Chang, H. S., Han, B., Zhu, T., Wang, X., Kreps, J. A., and Kay, S. A. (2000) Orchestrated transcription of key pathways in *Arabidopsis* by the circadian clock, *Science 290*, 2110−2113.
19. Wilde, A., Mikolajczyka, S., Alawady, A., Lokstein, H., and Grimm, B. (2004) The *gun4* gene is essential for cyanobacterial porphyrin metabolism, *FEBS Lett. 5*, 119−123.
20. Zhang, J., and Madden, T. L. (1997) PowerBLAST: A new network BLAST application for interactive or automated sequence analysis and annotation, *Genome Res. 7*, 649−656.
21. Servant, F., Bru, C., Carrere, S., Courcelle, E., Gouzy, J., Peyruc, D., and Kahn, D. (2002) ProDom: Automated clustering of homologous domains, *Briefings Bioinf. 3*, 246−251.
22. Bateman, A., Coin, L., Durbin, R., Finn, R. D., Hollich, V., Griffiths-Jones, S., Khanna, A., Marshall, M., Moxon, S., Sonnhammer, E. L. L., Studholme, D. J., Yeats, C., and Eddy, S. R. (2004) The Pfam protein families database, *Nucleic Acids Res. 32*, D138−D141.
23. Gibson, L. C. D., Jensen, P. E., and Hunter, C. N. (1999) Magnesium chelatase from *Rhodobacter sphaeroides*: initial characterization of the enzyme using purified subunits and evidence for a BchI-BchD complex, *Biochem. J. 337*, 243−251.
24. Jensen, P. E., Gibson, L. C. D., and Hunter, C. N. (1999) ATPase activity associated with the magnesium-protoporphyrin IX chelatase enzyme of *Synechocystis* sp. PCC6803: evidence for ATP hydrolysis during $Mg^{2+}$ insertion, and the MgATP-dependent interaction of the ChlI and ChlD subunits, *Biochem. J. 339*, 127−134.
25. Jensen, P. E., Gibson, L. C. D., Shephard, F., Smith, V., and Hunter, C. N. (1999) Introduction of a new branchpoint in tetrapyrrole biosynthesis in *Escherichia coli* by co-expression of genes encoding the chlorophyll-specific enzymes magnesium chelatase and magnesium protoporphyrin methyltransferase, *FEBS Lett. 455*, 349−354.
26. Shepherd, M., Reid, J. D., and Hunter, C. N. (2003) Purification and kinetic characterization of the magnesium protoporphyrin IX methyltransferase from *Synechocystis* PCC6803, *Biochem. J. 371*, 351−360.
27. Shepherd, M., and Hunter, C. N. (2004) Transient kinetics of the reaction catalysed by magnesium protoporphyrin IX methyltransferase, *Biochem. J. 382*, 1009−1013.
28. Ramakrishnan, V., Finch, J. T., Graziano, V., Lee, P. L., and Sweet, R. M. (1993) Crystal structure of globular domain of histone H5 and its implications for nucleosome binding, *Nature 362*, 219−223.
29. Otwinowski, Z. (1993) Oscillation data reduction program, in *Data Collection and Processing* (Sawyer, L., Isaacs, N., and Bailey, S., Eds.) pp 56−62, SERC Daresbury Laboratory, Warrington, U.K..
30. Terwilliger, T. C., and Berendzen, J. (1999) Automated MAD and MIR structure solution, *Acta Crystallogr., Sect. D: Biol. Crystallogr. 55*, 849−861.
31. Terwilliger, T. C. (2000) Maximum-likelihood density modification, *Acta Crystallogr., Sect. D: Biol. Crystallogr. 56*, 965−972.
32. Murshudov, G. N., Vagin, A. A., and Dodson, E. J. (1997) Refinement of macromolecular structures by the maximum-likelihood method, *Acta Crystallogr., Sect. D: Biol. Crystallogr. 53*, 240−255.
33. Bailey, S. (1994) The CCP4 Suite—Programs for protein crystallography, *Acta Crystallogr., Sect. D: Biol. Crystallogr. 50*, 760−763.
34. Alawady, A. E., and Grimm, B. (2005) Tobacco Mg protoporphyrin IX methyltransferase is involved in inverse activation of Mg porphyrin and protoheme synthesis, *Plant J. 41*, 282−290.

BI050240X